Physics Letters B 697 (2011) 194–198

Contents lists available at ScienceDirect

Physics Letters B

www.elsevier.com/locate/physletb

Polarization observables in deuteron photodisintegration below 360 MeV

J. Glister [a,b,*,1], G. Ron [c,2], B.W. Lee [d], R. Gilman [e,f], A.J. Sarty [a], S. Strauch [g], D.W. Higinbotham [e], E. Piasetzky [c], K. Allada [h], W. Armstrong [i], J. Arrington [j], H. Arenhövel [k], A. Beck [l], F. Benmokhtar [m], B.L. Berman [n], W. Boeglin [o], E. Brash [p], A. Camsonne [e], J. Calarco [q], J.P. Chen [e], S. Choi [d], E. Chudakov [e], L. Coman [r], B. Craver [r], F. Cusanno [s], J. Dumas [f], C. Dutta [h], R. Feuerbach [e], A. Freyberger [e], S. Frullani [s], F. Garibaldi [s], J.-O. Hansen [e], T. Holmstrom [t], C.E. Hyde [u,v], H. Ibrahim [u,w], Y. Ilieva [n], C.W. de Jager [e], X. Jiang [f], M.K. Jones [e], Hyekoo Kang [d], A. Kelleher [x], E. Khrosinkova [y], E. Kuchina [f], G. Kumbartzki [f], J.J. LeRose [e], R. Lindgren [r], P. Markowitz [o], S. May-Tal Beck [l], E. McCullough [a,3], D. Meekins [e], M. Meziane [x], Z.-E. Meziani [i], R. Michaels [e], B. Moffit [x], B.E. Norum [r], Y. Oh [d], M. Olson [z], M. Paolone [g], K. Paschke [r], C.F. Perdrisat [x], M. Potokar [aa], R. Pomatsalyuk [e,ab], I. Pomerantz [c], A. Puckett [ac], V. Punjabi [ad], X. Qian [ae], Y. Qiang [ac], R.D. Ransome [f], M. Reyhan [f], J. Roche [af], Y. Rousseau [f], A. Saha [e], B. Sawatzky [r,i], E. Schulte [f], M. Schwamb [k], M. Shabestari [r], A. Shahinyan [ag], R. Shneor [c], S. Širca [aa], K. Slifer [r], P. Solvignon [j], J. Song [d], R. Sparks [e], R. Subedi [y], G.M. Urciuoli [s], K. Wang [r], B. Wojtsekhowski [e], X. Yan [d], H. Yao [i], X. Zhan [ac], X. Zhu [ae]

[a] *Saint Mary's University, Halifax, Nova Scotia B3H 3C3, Canada*
[b] *Dalhousie University, Halifax, Nova Scotia B3H 3J5, Canada*
[c] *Tel Aviv University, Tel Aviv 69978, Israel*
[d] *Seoul National University, Seoul 151-747, Republic of Korea*
[e] *Thomas Jefferson National Accelerator Facility, Newport News, VA 23606, USA*
[f] *Rutgers, The State University of New Jersey, Piscataway, NJ 08855, USA*
[g] *University of South Carolina, Columbia, SC 29208, USA*
[h] *University of Kentucky, Lexington, KY 40506, USA*
[i] *Temple University, Philadelphia, PA 19122, USA*
[j] *Argonne National Laboratory, Argonne, IL 60439, USA*
[k] *Institut für Kernphysik, Johannes Gutenberg-Universität, D-55099 Mainz, Germany*
[l] *NRCN, P.O. Box 9001, Beer-Sheva 84190, Israel*
[m] *University of Maryland, Baltimore, MD, USA*
[n] *George Washington University, Washington, DC 20052, USA*
[o] *Florida International University, Miami, FL 33199, USA*
[p] *Christopher Newport University, Newport News, VA 23606, USA*
[q] *University of New Hampshire, Durham, NH 03824, USA*
[r] *University of Virginia, Charlottesville, VA 22094, USA*
[s] *INFN, Sezione Sanitá and Istituto Superiore di Sanitá, Laboratorio di Fisica, I-00161 Rome, Italy*
[t] *Longwood University, Farmville, VA 23909, USA*
[u] *Old Dominion University, Norfolk, VA 23508, USA*
[v] *Université Blaise Pascal / CNRS-IN2P3, F-63177 Aubière, France*
[w] *Cairo University, Giza 12613, Egypt*
[x] *College of William and Mary, Williamsburg, VA 23187, USA*
[y] *Kent State University, Kent, OH 44242, USA*
[z] *Saint Norbert College, Greenbay, WI 54115, USA*
[aa] *Jožef Stefan Institute, 1000 Ljubljana, Slovenia*
[ab] *NSC Kharkov Institute of Physics and Technology, Kharkov 61108, Ukraine*
[ac] *Massachusetts Institute of Technology, Cambridge, MA 02139, USA*
[ad] *Norfolk State University, Norfolk, VA 23504, USA*
[ae] *Duke University, Durham, NC 27708, USA*
[af] *Ohio University, Athens, OH 45701, USA*
[ag] *Yerevan Physics Institute, Yerevan 375036, Armenia*

* Corresponding author.
E-mail address: jglister@jlab.org (J. Glister).

0370-2693/$ – see front matter
doi:10.1016/j.physletb.2011.01.061

ARTICLE INFO

Article history:
Received 28 October 2010
Received in revised form 16 January 2011
Accepted 27 January 2011
Available online 3 February 2011
Editor: D.F. Geesaman

Keywords:
Deuteron photodisintegration
Polarization
Meson–baryon model

ABSTRACT

High precision measurements of induced and transferred recoil proton polarization in $d(\vec{\gamma},\vec{p})n$ have been performed for photon energies of 277–357 MeV and $\theta_{cm} = 20°$–$120°$. The measurements were motivated by a longstanding discrepancy between meson–baryon model calculations and data at higher energies. At the low energies of this experiment, theory continues to fail to reproduce the data, indicating that either something is missing in the calculations and/or there is a problem with the accuracy of the nucleon–nucleon potential being used.

The conventional nuclear model uses baryon and meson degrees of freedom to describe nuclear structure and reactions. While this approach has been broadly successful for low-energy phenomena, it is widely believed that it will break down at high energies. Meson–baryon model (MBM) calculations require high precision NN potentials which are used to describe the finite spatial extent of hadrons [1] and contain free parameters fit to experimental NN scattering data. MBM calculations have been quite successful below excitation energies of a few hundred MeV in describing cross-section and polarization observables for electromagnetic reactions involving small nuclear systems [2–5].

In the few GeV energy region, cross-section measurements of the deuteron photodisintegration reaction [6] were found to approximately scale according to the constituent counting rules [7–9], predictions based on quark degrees of freedom. Also, quark models such as the quark–gluon string (QGS) [10,11] and hard rescattering (HR) [12] have been moderately successful in describing $d(\vec{\gamma},\vec{p})n$ polarization observables above ~ 1 GeV [13,14].

Small nuclear systems, such as the deuteron and ^{3}He, provide a useful testing ground for MBM calculations as they allow for reliable theoretical calculations. Electromagnetic probes of these small systems are useful since the weak coupling constant allows for perturbative methods to be used. Furthermore, polarization measurements in electron– and photon–deuteron reactions allow for a detailed study as they are sensitive to small amplitudes and effects. Since the beginning of polarization measurements, over 70 publications have presented over 1200 polarization data points for photodisintegration and the time-reversed radiative capture reaction. These data have been very useful in constraining and testing low energy MBM calculations. In order to test the upper limit in energy of the meson–baryon model, experiments and calculations have been extended to higher and higher energies. As the energy and momentum transfer increase, the distance scale probed decreases and one would expect that at some point the sub-nucleonic degrees of freedom would have to be considered.

The most advanced MBM calculation for $d(\vec{\gamma},\vec{p})n$ in the few hundred MeV region comes from Schwamb and Arenhövel [15–17,2]. They have included meson-exchange currents, final-state interactions, relativistic corrections and a modern baryon–baryon potential in a non-relativistic field theory with nucleon, meson and Δ degrees of freedom. Free parameters are constrained by fits to NN scattering, πN scattering and pion photoproduction data [15]. Up to excitation energies of roughly 500 MeV, there is generally good agreement between their calculations and data for the differential cross-section, the cross-section asymmetry for linearly polarized photons (Σ) and the polarized target asymmetry (T). However, a striking disagreement emerges between 300 and 500 MeV, where the induced recoil proton polarization (P_y) at $\theta_{cm} = 90°$ is predicted to approach zero with increasing energy, yet the data grow in magnitude to nearly -1 at 500 MeV. Kang et al. [18] developed a model for $d(\vec{\gamma},\vec{p})n$ using a diagrammatic method which predicted a large magnitude of P_y above 300 MeV. They considered π, ρ, η and ω meson exchanges and 17 well-established nucleon and Δ resonances with a mass less than 2 GeV and $J \leqslant 5/2$, with all resonance parameters taken from the Particle Data Group [19]. However, the work cannot be validated as it was not published, it did not include channel coupling or consider final-state interactions completely (by solving the Schrödinger equation with an NN potential) and failed to describe the large induced polarization seen at ~ 500 MeV [13]. The pre-existing data between 300 and 500 MeV consist mainly of induced polarization measurements taken at different labs (with good angular distributions at only a few energies), Σ cross-section asymmetry measurements [20–23], along with a recent set of tensor analyzing powers [24] spanning 25–600 MeV. Also, no data of polarization transfer for circularly polarized photons had been taken below 500 MeV. We obtained a systematic set of the induced recoil polarization observables between 277 and 357 MeV in order to identify where in energy the measurements and the existing calculations begin to diverge. Benchmark measurements of transferred recoil polarization were also taken in this energy region to further constrain the theory. The polarization observables are written as $(P_x^{c'}, P_y, P_z^{c'})$, where c' denotes transferred polarization due to a circularly polarized photon beam, $\hat{z}$ is along recoil proton momentum in the center-of-mass frame, $\hat{y}$ is perpendicular to the reaction plane in the center-of-mass frame and $\hat{x} = \hat{y} \times \hat{z}$. Note that $P_x^{c'}$ and $P_z^{c'}$ are sometimes denoted as C_x and C_z, as in [13]. $P_x^{c'}$ and P_y are the real and imaginary parts of the same combination of amplitudes, so a measurement of both fully determines this amplitude combination.

The experiment was carried out in Hall A of Jefferson Lab [25]. A continuous electron beam with longitudinal polarization ranging from 80–85% was produced using a strained gallium–arsenide (GaAs) source [26,27]. The longitudinal polarization in Hall A was limited to 38–41% due to multi-hall running. The beam helicity was flipped pseudo-randomly at 30 Hz, with negligible difference in total beam charge between the two helicity states. The electron beam, with energy 362 MeV, was incident on a copper radiator with thicknesses of 3, 4 or 5% of a radiation length. The outgoing (untagged) circularly polarized Bremsstrahlung photons were incident on a 15 cm long liquid deuterium target. The ratio of photon to electron polarization varied from 80 to near 100% and was calculated on an event-by-event basis using the formula found in [28].

[1] Present address: TRIUMF, 2004 Westbrook Mall, Vancouver, BC V6T 2A3, Canada.
[2] Present address: Lawrence Berkeley National Laboratory, Berkeley, CA 94720, USA.
[3] Present address: University of Western Ontario, London, Ontario N6A 3K7, Canada.

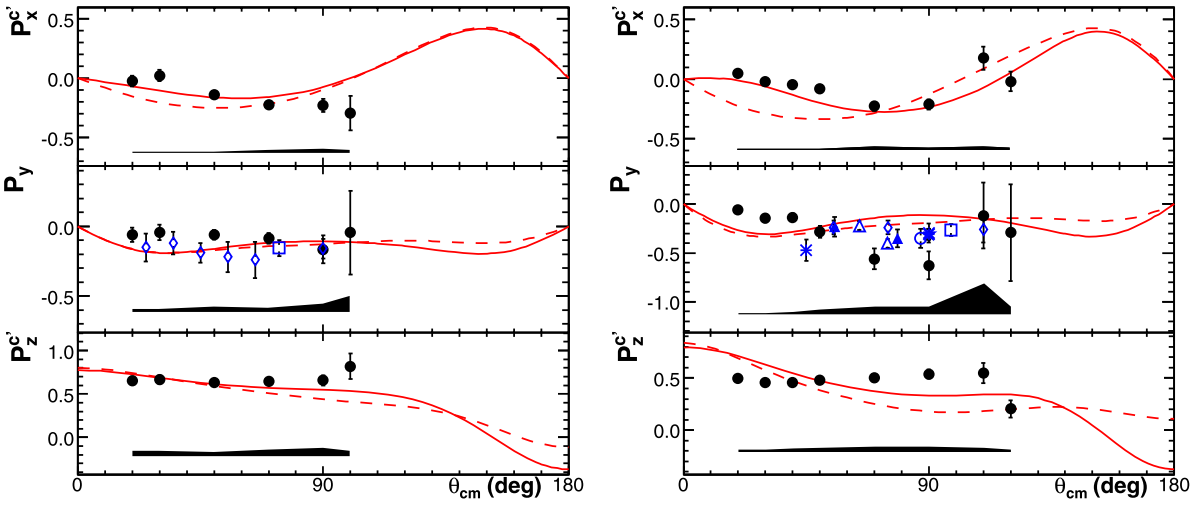

Fig. 1. (Color online.) Angular distributions of the recoil proton polarizations in $d(\vec{\gamma},\vec{p})n$, for $E_\gamma = 277 \pm 10$ MeV (left-hand side) and $E_\gamma = 357 \pm 10$ MeV (right-hand side). Error bars are statistical only; systematic uncertainties are shown as black bands. The solid line is the Schwamb and Arenhövel calculation [15–17,2]. The dashed line is a recent improvement from [36]. Present data are denoted by the filled circles and previous P_y data are from Stanford (filled triangles) [37], Bonn (open squares) [38], Tokyo (open circles) [39], Yerevan (open triangles) [40] and Kharkov (asterisks [41–43], filled stars [44], open diamonds [45]). Note that there are two overlapping P_y measurements with different uncertainties for $E_\gamma = 277$ MeV and $\theta_{cm} = 90°$.

The protons were detected in the left High Resolution Spectrometer (HRS) [29], made up of one dipole and three quadrupole magnets. The vertical drift chambers, or VDCs, were used to track the protons after the magnetic field of the dipole. The HRS optics matrix was used to reconstruct the scattering angles, momentum and positions at the target. Triggering and time-of-flight information was provided by two planes of plastic scintillators, S1 and S2.

The Focal Plane Polarimeter (FPP), downstream of the VDCs and trigger panels, is used to determine the recoil polarization of the protons by measuring a secondary scattering of the protons with a ~ 1.7 g/cm^3 carbon analyzer, where the spin–orbit coupling between the transverse proton spin and the orbital angular momentum about the carbon nucleus leads to an asymmetry in the azimuthal scattering angle, ϕ_{fpp}. The spin–orbit force is insensitive to the longitudinal component of proton spin at the focal plane. GEANT [30] Monte Carlo studies were used to determine the optimal analyzer thickness for each kinematic setting (varied from 0.75″ to 3.75″). The transferred and induced proton polarizations at the focal plane were extracted using the maximum likelihood method taking into account the beam helicity state for each event [13]. The focal plane polarizations were transported back to the target using COSY [31], a differential algebra based code. Spin transport of the beam polarization dependent (independent) proton focal plane polarizations gives access to the beam polarization dependent (independent) target polarizations $P_x^{c'}$ and $P_z^{c'}$ (P_y). A detailed description of the polarimeter can be found in [32,33].

The experiment covered an angular range of $\theta_{cm} = 20°$–$120°$, generally in 10° steps, although some intermediate angles were skipped due to time constraints. Five 20 MeV bins in photon energy spanning 277–357 MeV (bin center) were covered at each center-of-mass angle using two spectrometer momentum settings, except at the three largest angles and one of the intermediate ones. In all measurements the proton had sufficient momentum to exclude the existence of a pion in the final state. Background due to electrodisintegration reactions and interactions with the target walls was subtracted using a method similar to previous photodisintegration experiments [13].

The FPP was calibrated with ep elastic scattering [34], which determines the false asymmetry and the analyzing power [35], the strength of the spin-dependent p–C interaction. False asymmetries, caused by chamber misalignments and inhomogeneities in detector efficiency, cancel to first order for polarization transfer but remain for the induced polarization. The FPP chambers were aligned both internally and to the VDCs using straight-through trajectories, with the analyzer block removed. The remaining false asymmetries were parameterized as a Fourier series and subtracted out.

The angular dependence of the present transferred ($P_x^{c'}$ and $P_z^{c'}$) and induced (P_y) polarization data are shown as filled circles in Fig. 1 for photon energies of 277 MeV (left-hand side) and 357 MeV (right-hand side). Previous induced polarization measurements [37–46] are also shown, where uncertainty bars are statistical only, except for the Tokyo measurements (open circles) [39] which have bars representing both statistical and systematic uncertainties. The uncertainty bars for the present measurements are statistical only; systematic uncertainties are shown as black bands. The systematic uncertainties include uncertainties in beam energy, polarization and position, false asymmetry and analyzing power parameterizations, spin transport, momentum, and FPP angular resolution. The spin transport systematic analysis was similar to that of a previous work [32]. Absolute statistical (systematic) uncertainties for $P_x^{c'}$, P_y and $P_z^{c'}$ ranged from 0.01–0.15 (0.01–0.04), 0.01–0.50 (0.01–0.33) and 0.01–0.15 (0.02–0.10), respectively. The largest contribution to the systematic uncertainty for both $P_x^{c'}$ and $P_z^{c'}$ was the analyzing power parameterization while the largest contribution for P_y was the false asymmetry parameterization.

Our P_y data at 70° and 90° for $E_\gamma = 357$ MeV are larger in magnitude than previous results. We are in a region where there is the start of a strong energy dependence and small cross-sections. Measurements covered different energy ranges. As a results of this, older measurements suffered from large backgrounds and poor consistency. This was seen previously [13]. The trend of P_y in our data at 90° is consistent with higher energy measurements, and our P_y results cannot be changed independently of the polarization transfer data.

The solid line is the Schwamb and Arenhövel calculation [15–17,2]. The dashed line is a recent refinement from [36], which includes several technical advances such as a non-perturbative treatment of the πNN dynamics (as opposed to an approximate treatment). The new calculation fulfills unitarity to leading order,

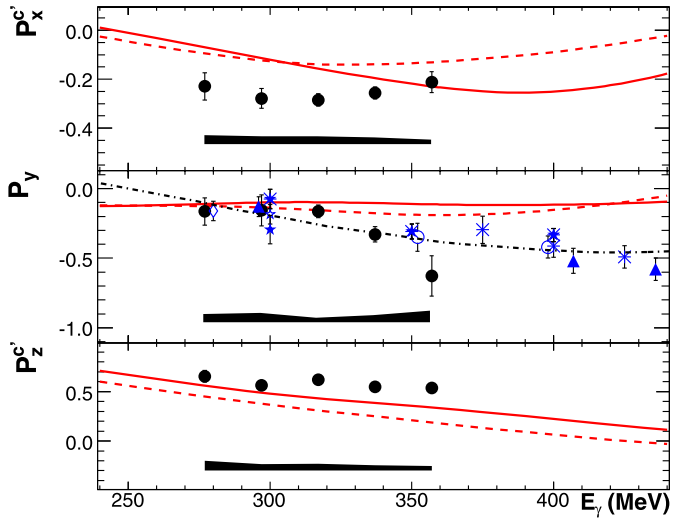

Fig. 2. (Color online.) Energy distribution of the recoil proton polarization in $d(\vec{\gamma},\vec{p})n$ for $\theta_{cm} = 90°$. Error bars are statistical only; systematic uncertainties are shown as black bands. The solid line is the Schwamb and Arenhövel calculation [15–17,2], the dashed line is a recent improvement from [36] and the dashed-dotted curve is the Kang et al. calculation [18]. Present data are denoted by the filled circles and previous P_y data are from Stanford (filled triangles) [37], Tokyo (open circles) [39] and Kharkov (asterisks [41–43], filled stars [44], open diamonds [45], open stars [46]).

requires fewer free parameters and is more rigorous from a conceptual point of view, as it considers seven reactions simultaneously in a coupled channel approach, rather than only $\gamma d \to pn$ and $NN \to NN$.

The calculations of Schwamb and Arenhövel describe fairly well the transferred polarizations, $P_x^{c'}$ and $P_z^{c'}$. At the lowest energy, these calculations are also in good agreement with the induced polarization, P_y, but at the higher energies the present data show a strong deviation from the theoretical predictions. The calculations also appear to overestimate the magnitude of P_y for small θ_{cm}, even at the lowest energy of 277 MeV. Since $P_x^{c'}$ and P_y are the real and imaginary parts of the same sum of amplitudes, the real part appears to be better predicted above the Δ resonance (dominant at roughly 300 MeV) while the imaginary part is better predicted at low energy, below the Δ resonance.

$P_z^{c'}$ arises from the combination of amplitudes squared and aside from the lowest energy the data exhibit a different angular dependence than both theoretical predictions. The disagreement may be due to something being inaccurately approximated in the calculations (*e.g.* the restriction to one-meson exchange). Also, free parameters in the potential, which enter into the final-state interactions, were fit to NN scattering data. Although the free parameters are well defined below pion threshold, only the dominant $^1D_2$ channel was described well above pion threshold [15]. Alternatively, QCD-inspired potentials, based on chiral perturbation theory (see [47] for a review), may have to be considered. However, these potentials are currently only considered up to the pion threshold, indicating a need for improved QCD-inspired potentials in the Δ-region.

The energy dependence at $\theta_{cm} = 90°$ is shown in Fig. 2 for photon energies of 280–480 MeV. The Kang et al. calculation for P_y is denoted by the dashed-dotted curve and describes the data well in this energy region but underestimates the magnitude of the highest energy point from the present measurements. The Schwamb and Arenhövel calculations (old and new denoted by solid and dashed lines, respectively) predict P_y to remain relatively flat and near zero below 500 MeV, whereas the present P_y results reach a value of $-0.63 \pm 0.14 \pm 0.09$ by 357 MeV. Beyond an energy of roughly 320 MeV, the Schwamb and Arenhövel calculations are unable to describe the present P_y measurements. The increasingly poor agreement for P_y as the energy is raised may be due to tails of higher lying resonances. Within the impulse approximation, it was found that neither the D_{13} (invariant mass $W = 1520$ MeV) nor S_{11} ($W = 1535$ MeV) resonances played significant roles in P_y below 400 MeV [48]. However, a coupled channel approach involving the D_{13} and S_{11} as well as the Roper resonance (P_{11} with $W = 1440$ MeV) and possibly a double Δ excitation (both of which were included approximately within the impulse approximation in [48]) may have to be considered.

Note that the old and present calculations are roughly equivalent, aside from a divergence at the highest energies for the polarization transfer $P_x^{c'}$, where the old calculation more closely resembles the data. The new calculation (dashed line) gives a slightly better description of P_y while the old calculation (solid line) more accurately describes $P_z^{c'}$. A similar situation was observed [24] for the deuteron photodisintegration tensor analyzing powers (T_{20}, T_{21} and T_{22}), where it was found that the new calculation was better at describing T_{20} and T_{22} but worse at describing T_{21}. Neither the old nor new calculations describe the energy dependence of $P_x^{c'}$ at $\theta_{cm} = 90°$, except for the agreement at 357 MeV between the present data and the old calculation. The overall shape of $P_z^{c'}$ as a function of energy appears to be modeled well, but the magnitude is underestimated by both calculations (more-so by the new model).

To summarize, we have provided new induced and transferred recoil proton polarization measurements for deuteron photodisintegration over a range of energies and angles. The present induced polarization measurements are consistent with theoretical predictions and previous measurements at all but the highest energies, where the most technically advanced MBM calculations appear unable to describe the large value of P_y. $P_x^{c'}$ appears to be described well using an old MBM calculation at the highest energy while $P_z^{c'}$ agrees with the same calculation (within uncertainties) at the lowest energy. It may be possible to remedy the situation by improving the fits of NN scattering partial waves above pion threshold, including higher mass resonances in a coupled channel approach or extending the calculation beyond the one-meson approximation. These present measurements should provide input for important tests to the state-of-the-art meson–baryon model calculations above pion threshold and it will be interesting to see whether the issue can be resolved or if other models (based on chiral perturbation theory, for instance) should be considered.

Acknowledgements

We thank the Jefferson Lab physics and accelerator divisions for their contributions. This work was supported by the US Department of Energy (including contract DE-AC02-06CH11357), the US National Science Foundation, the Israel Science Foundation, the Korea Science Foundation, the US–Israeli Bi-National Scientific Foundation, the Natural Sciences and Engineering Research Council of Canada, the Killam Trusts Fund, the Walter C. Sumner Foundation and the Deutsche Forschungsgemeinschaft (SFB 443). Jefferson Science Associates operates the Thomas Jefferson National Accelerator Facility under DOE contract DE-AC05-06OR23177. The polarimeter was funded by the US National Science Foundation, grants PHY 9213864 and PHY 9213869.

References

[1] R. Machleidt, K. Holinde, C. Elster, Phys. Rep. 149 (1987) 1.
[2] H. Arenhövel, E.M. Darwish, A. Fix, M. Schwamb, Mod. Phys. Lett. A 18 (2003) 190.

[3] L.E. Marcucci, M. Viviani, R. Schiavilla, A. Kievsky, S. Rosati, Phys. Rev. C 72 (2005) 014001.
[4] H. Arenhövel, M. Sanzone, in: Few Body Syst., Suppl., vol. 3, Springer, 1991.
[5] J. Carlson, R. Schiavilla, Rev. Mod. Phys. 70 (1998) 743.
[6] M. Mirazita, et al., Phys. Rev. C 70 (2004) 014005, and references within.
[7] S.J. Brodsky, G.R. Farrar, Phys. Rev. Lett. 31 (1973) 1153.
[8] V.A. Matveev, R.M. Muradian, A.N. Tavkhelidze, Nuovo Cimento Lett. 7 (1973) 719.
[9] P. Rossi, et al., Phys. Rev. Lett. 94 (2005) 012301.
[10] V.Y. Grishina, et al., Eur. Phys. J. A 18 (2003) 207.
[11] V.Y. Grishina, et al., Eur. Phys. J. A 19 (2004) 117.
[12] M.M. Sargsian, Phys. Lett. B 587 (2004) 41.
[13] K. Wijesooriya, et al., Phys. Rev. Lett. 86 (2001) 2975, and references within.
[14] X. Jiang, et al., Phys. Rev. Lett. 98 (2007) 182302.
[15] M. Schwamb, H. Arenhövel, Nucl. Phys. A 690 (2001) 647.
[16] M. Schwamb, H. Arenhövel, Nucl. Phys. A 690 (2001) 682.
[17] M. Schwamb, H. Arenhövel, Nucl. Phys. A 696 (2001) 556.
[18] Y. Kang, et al., Abstracts of the Particle and Nuclear Intersections Conference, MIT, Cambridge, MA, 1990.
[19] C. Amsler, et al., Phys. Lett. B 667 (2008) 1.
[20] V.G. Gorbenko, Y.V. Zhebrovsky, L.Y. Kolesnikov, A.L. Rubashkin, P.V. Sorokin, Nucl. Phys. A 381 (1982) 330.
[21] F.V. Adamian, et al., J. Phys. G 17 (1991) 1189.
[22] G. Blanpied, et al., Phys. Rev. C 61 (1999) 024604.
[23] S. Wartenberg, et al., Few Body Syst. 26 (1999) 213.
[24] I.A. Rachek, et al., Phys. Rev. Lett. 98 (2007) 182303.
[25] C.W. Leemann, D.R. Douglas, G.A. Krafft, Annu. Rev. Nucl. Part. Sci. 51 (2001) 413.
[26] C.K. Sinclair, et al., Phys. Rev. ST Accel. Beams 10 (2007) 023501.
[27] C. Hernandez-Garcia, M.L. Stutzman, P.G. O'Shea, Phys. Today 61 (2) (2008) 44.
[28] H. Olsen, L.C. Maximon, Phys. Rev. 114 (1959) 887.
[29] J. Alcorn, et al., Nucl. Instrum. Methods A 522 (2004) 294.
[30] S. Agostinelli, et al., Nucl. Instrum. Methods A 506 (2003) 250.
[31] M. Berz, H. Hoffmann, H. Wollnik, Nucl. Instrum. Methods A 258 (1987) 402.
[32] V. Punjabi, et al., Phys. Rev. C 71 (2005) 055202.
[33] M. Jones, et al., in: T. Donnelly (Ed.), Abstracts of the Particle and Nuclear Intersections Conference, AIP, New York, 1997, p. 342.
[34] G. Ron, et al., Phys. Rev. Lett. 99 (2007) 202002.
[35] J. Glister, et al., Nucl. Instrum. Methods A 606 (2009) 578.
[36] M. Schwamb, Phys. Rep. 485 (2010) 109.
[37] F.F. Liu, D.E. Lundquist, B.H. Wiik, Phys. Rev. 165 (1968) 1478.
[38] R. Kose, B. Martin, R. Runkel, H. Wahlen, K.H. Kissler, Z. Phys. 220 (1969) 305.
[39] T. Kamae, et al., Nucl. Phys. B 139 (1978) 394.
[40] R.O. Avakyan, et al., Sov. J. Nucl. Phys. 52 (1990) 396.
[41] A.S. Bratashevskii, et al., Sov. J. Nucl. Phys. 31 (1980) 444.
[42] A.S. Bratashevskii, et al., Sov. J. Nucl. Phys. 32 (1980) 216.
[43] A.S. Bratashevskii, et al., Sov. J. Nucl. Phys. 43 (1986) 499.
[44] V.P. Barannik, et al., Nucl. Phys. A 451 (1986) 751.
[45] A.A. Zybalov, O.G. Konovalov, S.V. Marekhin, P.V. Sorokin, Y.O. Storozhenko, A.E. Tenishev, Nucl. Phys. A 533 (1991) 642.
[46] V.B. Ganenko, et al., Z. Phys. A 341 (1992) 205.
[47] A. Schwenk, Nucl. Phys. A 827 (2009) 161c.
[48] M. Schwamb, H. Arenhövel, P. Wilhelm, Few Body Syst. 19 (1995) 121.